Journal of Modern Optics
Publication details, including instructions for authors and subscription information:
http://www.tandfonline.com/loi/tmop20

The Quantum Electrodynamics of Synergistic Two-photon Processes

D.L. Andrews [a] & N.P. Blake [a]
[a] School of Chemical Sciences , University of East Anglia , Norwich, NR4 7TJ, England
Published online: 01 Mar 2007.

To cite this article: D.L. Andrews & N.P. Blake (1990) The Quantum Electrodynamics of Synergistic Two-photon Processes, Journal of Modern Optics, 37:4, 701-718, DOI: 10.1080/09500349014550771

To link to this article: http://dx.doi.org/10.1080/09500349014550771

JOURNAL OF MODERN OPTICS, 1990, VOL. 37, NO. 4, 701–718

The quantum electrodynamics of synergistic two-photon processes

D. L. ANDREWS and N. P. BLAKE
School of Chemical Sciences, University of East Anglia, Norwich NR4 7TJ, England

Abstract. In this paper it is demonstrated how the phenomena of cooperative Raman scattering and cooperative two-photon absorption may be described in a unified manner, through canonically transforming the system Hamiltonian. The unique features associated with the virtual photon coupling between centres are discussed. In particular it is illustrated how in the near-zone, close proximity leads to two-body two-photon events involving interaction-induced dipoles. In the far-zone, it is shown how the coupling between molecules may be understood in terms of a radiative dipole effect. Attention is focused upon the behaviour of this coupling for distributive and cooperative mechanisms in fluids, and the relative importance of each process discussed, particularly with regard to their very different range dependences. A detailed analysis of the coupling reveals that in two-photon absorption the distributive mechanism dominates, whilst in Raman scattering cooperative energy transfer is favoured. Finally recent progress in the field of synergism is reviewed along with the characteristics associated with synergism in Raman scattering and two-photon absorption.

1. Introduction

Conventional theories of two-photon inelastic light scattering and two-photon absorption are generally based on the assumption that the signal from a fluid or molecular crystal results from a simple superposition of signals from individual molecules, subject to local field corrections. Nonetheless it is well known that in single-photon absorption the interaction of atoms or molecules irradiated with light of a suitable frequency can result in the simultaneous excitation of two distinct species. The first observations of this effect were made in infrared studies on compressed gases, though recent work has mostly focused on interaction-induced *optical* transitions in gases and crystals.

In condensed matter, other cooperative effects are known to occur in connection with the photoproduction of relatively long-lived triplet states, either in individual molecules in the case of liquids, or in triplet excitons in crystalline solids. Because of their long lifetimes, the concentrations of such species can build up to a point where triplet–triplet annihilation ensues, either by molecular diffusion or by exciton migration [1], resulting in the generation of highly excited states decaying through short-wavelength luminescence. These processes often have a quadratic dependence on irradiance, and thus exhibit features characteristic of two-photon absorption. However, since the separate photon absorption processes and also the subsequent triplet–triplet annihilation are uncorrelated, such phenomena cannot be regarded as genuine multiphoton processes. Where singlet states are concerned, lifetimes are generally too short for concentrations to build up to a point where collisional annihilation is significant, if conventional irradiation sources are employed. With laser light of sufficient intensity, however, such effects are indeed observable.

0950-0340/90 $3·00

Laser excitation also provides the means for observing nonlinear optical effects involving the interaction of two or more photons with each atomic or molecular pair. The theoretical prediction of such a process was first made by Rios Leite and De Araujo (1980) in a paper concerned with cooperative absorption by atom pairs in solids [2]. However the first experimental observation made shortly afterwards by White (1981) [3] came from laser excitation studies of gaseous mixtures of barium and thallium. Atoms of both species were found to be simultaneously promoted to excited states by a concerted process involving the pairwise absorption of laser photons.

Recently, a number of new types of optical synergism involving two-photon processes have been the subject of renewed theoretical interest [4–8]. Here the two chemical centres which undergo concerted excitation may or may not be chemically similar, and can represent either distinct chromophores within a single molecule, loosely bound systems such as van der Waals molecules or solute particles within a coordination shell of solvent molecules, or else completely separate molecules. In the most general case, the two participating centres A and B undergo concerted excitation through either an elastic scattering process such as Stokes–Raman scattering, figure 1 (*a*), or two-photon absorption, figure 1 (*b*). The two processes are thus characterized by the absorption of one photon $\hbar\omega_1$, and either the emission or absorption of a second photon $\hbar\omega_2$. In general the process can be represented by the equation

$$\mathrm{A}+\mathrm{B}+\hbar\omega_1 \pm \hbar\omega_2 \rightarrow \mathrm{A}^*+\mathrm{B}^*. \tag{1}$$

For the purposes of the calculations presented below it is assumed that both molecules A and B are initially in their ground states, and that they are promoted during the synergistic process to excited vibrational or vibronic states designated by the asterisks in equation (1), and labelled α and β respectively. Then equation (1) is restricted only by the energy conservation requirement

$$E_{\alpha 0}+E_{\beta 0}=\hbar\omega_1 \pm \hbar\omega_2. \tag{2}$$

In the case of two-photon absorption, two types of synergistic absorption are of special interest. These are distinguished by whether the photons absorbed have the same, or different frequencies. The latter condition is in most cases determined by whether a single laser beam or two laser beams are employed for the excitation. In single-beam bimolecular photoabsorption the two absorbed photons have the same frequency and it is the synergistic interaction between two *non-identical* centres that is of interest. This interaction provides the mechanism for energy exchange such that an overall process;

$$\mathrm{A}+\mathrm{B}+2\hbar\omega \rightarrow \mathrm{A}^*+\mathrm{B}^*$$

can take place even when the individual transitions $\mathrm{A}\rightarrow\mathrm{A}^*$ and $\mathrm{B}\rightarrow\mathrm{B}^*$ are forbidden on energy grounds. From a phenomenological viewpoint, the process therefore has the characteristics of *mean-frequency* photoabsorption.

In the other case of interest the two centres have identical chemical composition and are excited by the absorption of two different photons, as for example from two different laser beams with frequencies ω_1 and ω_2. This process can be represented by the equation

$$\mathrm{A}+\mathrm{A}+\hbar\omega_1+\hbar\omega_2 \rightarrow \mathrm{A}^*+\mathrm{A}^*.$$

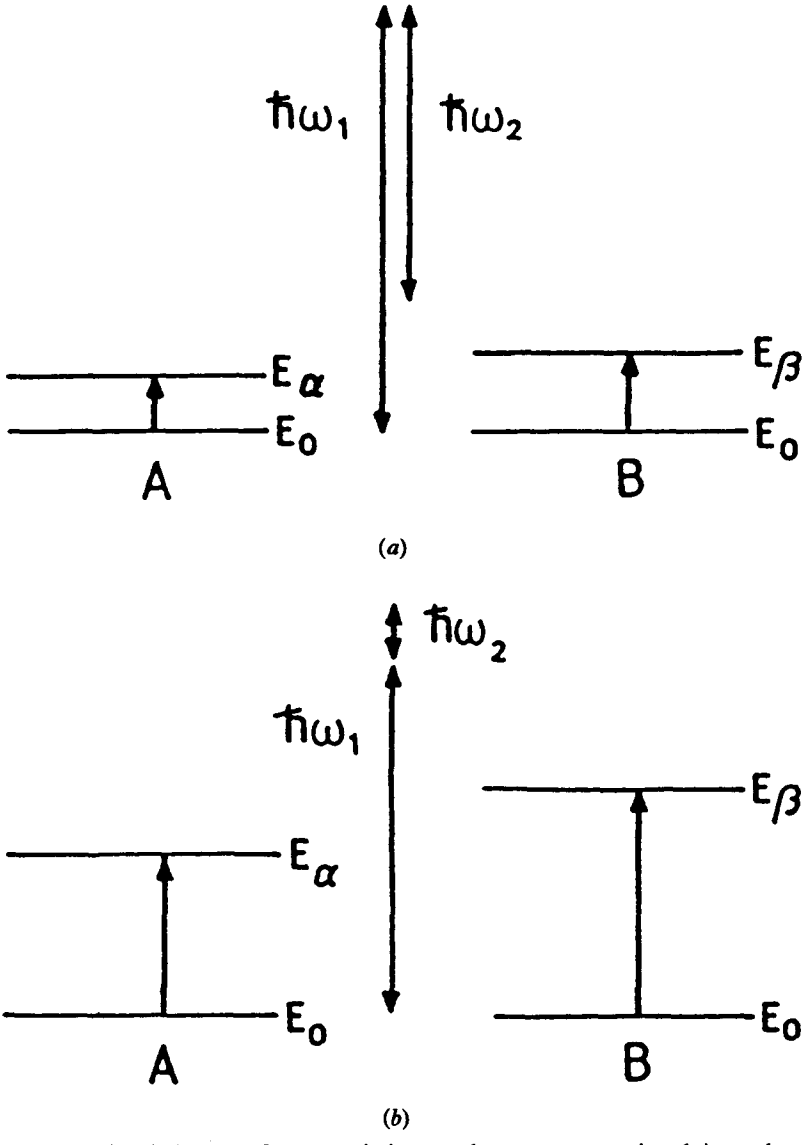

Figure 1. Energy level diagrams for synergistic two-photon processes involving a chemically inequivalent molecular pair A, B: (*a*) Stokes–Raman scattering, and (*b*) two-photon absorption.

This synergistic phenomenon again has the characteristics of mean-frequency absorption: here, however, it is the molecular excitation frequency which equals the mean of the two photon frequencies.

Synergism in Raman scattering allows for different vibrational modes to be excited at centres A and B. It is therefore characterized by the appearance of bimolecular combination bands in the spectrum, since the coupling itself places no constraints on the modes excited at each centre. In this case the observed combination frequencies cannot arise through any intermolecular mechanism, and

must be the result of synergistic Raman scattering. However if A and B are chemically identical, it is possible for identical modes to be excited at each site. This leads to vibrational harmonics in the Raman spectrum, even in the absence of any inherent anharmonicity in the corresponding vibration [8].

Each of the above-mentioned synergistic two-photon processes can in principle take place by one of two mechanisms. The first process, termed cooperative, corresponds to a case where both photons $\hbar\omega_1$ and $\hbar\omega_2$ interact with a different molecule as shown in figure 2 [9]. The second mechanism, termed distributive, describes a process in which both photon events occur in a single molecule as in figure 3 [10]. In each case, the energy mismatch for the molecular transitions is transferred by means of a virtual photon which couples with each molecule by electric-dipole coupling. However, important differences arise in the range-dependences of the two mechanisms. These differences, as is shown in section 3, hinge on the magnitude of the energy mismatch conveyed by the virtual photon. A detailed analysis of the coupling reveals that in two-photon absorption, it is the distributive mechanism that is dominant, whilst in Raman scattering cooperative energy transfer is favoured.

There is also a significant difference in the selection rules applying to the two types of process. In the cooperative case the two molecular transitions are separately allowed under well known Raman (two-photon) selection rules, since each molecule interacts with one real photon and either emits or absorbs a virtual photon. In the same way the distributive case provides for excitation through three- and one-photon allowed transitions, and may thus lead to excitation of states which are formally Raman- or two-photon forbidden. Since on the whole these processes are of most interest for molecules of fairly high symmetry, it can safely be assumed that in most cases one mechanism alone is involved in the excitation to a particular pair of excited states α and β. In the following section, a theory is developed for the former, cooperative, mechanism which relates to transitions allowed under the normal symmetry selection rules for two-photon absorption and Raman scattering. The corresponding theory for the distributive mechanism follows along very similar lines and has been discussed in detail elsewhere [6, 10]. The novel features which arise out of virtual photon coupling are essentially identical for both types of mechanism, and it is these which are subsequently examined in section 3.

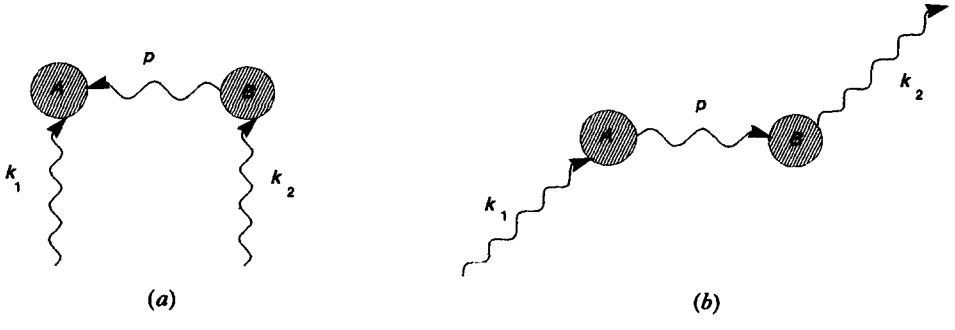

Figure 2. A schematic illustration of the two types of cooperative two-photon process involving the molecular centres A and B; (*a*) cooperative two-photon absorption, and (*b*) cooperative Raman scattering: **p** in this figure represents the propagator for virtual photon coupling.

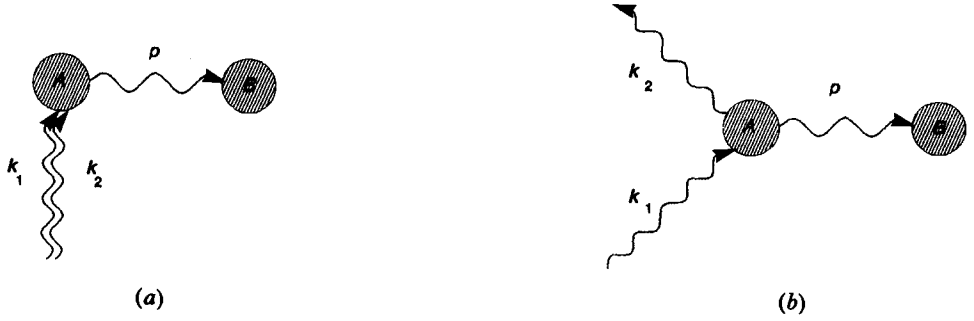

Figure 3. A schematic illustration of the two possible types of distributive two-photon process involving the molecular centres A and B; (*a*) two-photon absorption, and (*b*) Raman scattering.

2. The quantum electrodynamics of synergistic two-photon processes

In molecular quantum electrodynamics, the adoption of the Coulomb gauge with the multipolar interaction Hamiltonian of Power, Zienau and Woolley [11], leads to a description of molecular interactions in terms of a coupling associated with the creation and subsequent annihilation of virtual photons. All energy transferred between molecular centres is therefore mediated through the radiation field via virtual photons. As a consequence of this, the interactions which occur between charges in different molecules propagate with the speed of light. In the *near-zone*, virtual photon coupling is purely longitudinal with respect to the intermolecular separation vector **R**, and therefore has the characteristics of a static interaction in which the electron distribution of one molecule responds to the scalar field of the neighbouring centre. Thus in the electric-dipole approximation, the near-zone result is the familiar induced-dipole–induced-dipole result as obtained from the semi-classical calculations, see for example [12]. In the *far-zone*, the virtual photon that propagates between the centres takes on a real character, and the effect is essentially that of a radiative dipole.

The starting point for any calculation is construction of the probability amplitude connecting the initial and final states for the system. In the problem to be considered here, two interacting molecules, arbitrarily labelled A and B, are placed within the interaction volume of a laser beam, or beams. Initially, at time $t=0$, it is assumed that both molecules are in their ground states, $|0\rangle$. The calculation then proceeds to evaluate the probability that at a later time t, the molecules are synergistically excited to states $|\alpha\rangle$ and $|\beta\rangle$, via the annihilation of two photons (cooperative two-photon absorption), or the annihilation of one laser photon and creation of one scattered photon (cooperative Raman scattering). In the quantum electrodynamical representation of these processes the initial and final states $|\mathrm{i}\rangle$ and $|\mathrm{f}\rangle$ respectively are therefore defined as

$$|\mathrm{i}\rangle = |0; 0; \{n_1\}; \{n_2\}; 0\rangle, \tag{3}$$

$$|\mathrm{f}\rangle = |\alpha; \beta; \{(n_1 - 1)\}; \{(n_2 \mp 1)\}; 0\rangle. \tag{4}$$

Here the sequence in the ket denotes; | the state of A; the state of B; the number of photons in mode 1; the number of photons in mode 2; the number of virtual photons$\rangle$. For both cooperative Raman scattering (RS), and synergistic two-photon absorption (TPA), mode 1 refers to the mode of the laser radiation, with the curly

brackets denoting that a set of modes is to be used for multi-mode sources. Mode 2 however denotes distinctly different number states for the Raman scattering and two-photon absorption processes. In the former case, mode 2 is the mode of the scattered photon; in the final state the occupation number of this number state is increased by one. In the latter case, mode 2 is associated with a second laser, and consequently in the final state the occupation number of this mode is decreased by one. The coherence factor which marginally modifies the above treatment in the case where modes 1 and 2 are the same is discussed elsewhere [9, 10].

As noted above, intermolecular perturbations are described in terms of virtual photon coupling; thus for the processes under consideration here, four distinct radiation-molecule interactions occur within the time interval t. The probability amplitude, $c_{\mathrm{fi}}(t)$, for either process $|\mathrm{i}\rangle \rightarrow |\mathrm{f}\rangle$ defined in equations (3) and (4) can be therefore be calculated from

$$c_{\mathrm{fi}}(t) = \langle \mathrm{f}|\, U(t,0)\,|\mathrm{i}\rangle, \tag{5}$$

where the evolutionary operator $U(t, 0)$ for the process results from the fourth-order perturbation term in the Dyson equation [13] and is

$$U(t,0) = \frac{(\mathrm{i}\hbar)^{-4}}{4!} T\Bigg[\int_0^t \mathrm{d}t_1 \int_0^t \mathrm{d}t_2 \int_0^t \mathrm{d}t_3 \int_0^t \mathrm{d}t_4 \times H_{\mathrm{int}}^{\mathrm{A}}(\mathbf{k}, t_1) H_{\mathrm{int}}^{\mathrm{A}}(\mathbf{p}, t_2) H_{\mathrm{int}}^{\mathrm{B}}(\mathbf{p}, t_3) H_{\mathrm{int}}^{\mathrm{B}}(\mathbf{k}', t_4)\Bigg], \tag{6}$$

where T is the Dyson time-ordering operator. Here there is implicit summation over virtual photon modes, and polarization labels are dropped for brevity. The evolution operator describes how any stationary state of the initially unperturbed system (i.e. a state of the system in the absence of any time-dependent perturbation) evolves through time when the perturbation is 'switched on'. In the Heisenberg representation, the interaction Hamiltonian, in the electric-dipole approximation, has the explicit form

$$H_{\mathrm{int}}^{\xi}(\mathbf{k}, \lambda, t) = -\varepsilon_0^{-1} \boldsymbol{\mu}(\xi, t) \cdot \mathbf{d}^{\perp}(\mathbf{k}, \lambda, R_{\xi}, t), \tag{7}$$

where $\boldsymbol{\mu}(\xi)$ is the electric dipole moment operator for a molecule ξ at a position R_{ξ}, and $\mathbf{d}^{\perp}$ is the transverse electric displacement operator which, for the mode with propagation vector $\mathbf{k}$ (circular frequency $\omega = c|\mathbf{k}|$) and polarization λ, is given by

$$\mathbf{d}^{\perp}(\mathbf{k}, \lambda, \mathbf{r}, t) = \mathrm{i}(\hbar c k \varepsilon_0 / 2V)^{1/2} \times [\mathbf{e}^{(\lambda)}(\mathbf{k}) a^{(\lambda)}(\mathbf{k}, t) \exp(\mathrm{i}\mathbf{k}\cdot\mathbf{r}) - \bar{\mathbf{e}}^{(\lambda)}(\mathbf{k}) a^{\dagger(\lambda)}(\mathbf{k}, t) \exp(-\mathrm{i}\mathbf{k}\cdot\mathbf{r})]. \tag{8}$$

Here $\mathbf{e}^{(\lambda)}$ is a polarization vector in the direction of the electric field, $a^{(\lambda)}(\mathbf{k}, t)$, $a^{\dagger(\lambda)}(\mathbf{k}, t)$ are the normal photon annihilation and creation operators respectively, and $a^{(\lambda)}(\mathbf{k}, t) = a^{(\lambda)}(\mathbf{k}) \exp(-\mathrm{i}\omega t)$. To calculate the result for $c_{\mathrm{fi}}(t)$ explicitly requires the summing of all 24 time-orderings in equation (6). This calculation is facilitated by the use of time-ordered diagrams; figure 4 illustrates four typical contributions: (*a*) and (*b*) relate to TPA and (*c*) and (*d*) to RS.

In a recent paper [8], it has been illustrated how the derivation of the required probability amplitude is simplified if the system Hamiltonian is canonically transformed. In this procedure the original Hamiltonian undergoes a unitary transformation in Hilbert space. This transformation eliminates the lowest-order interaction terms, and the remaining lowest order interactions, denoted by H_{eff}, are

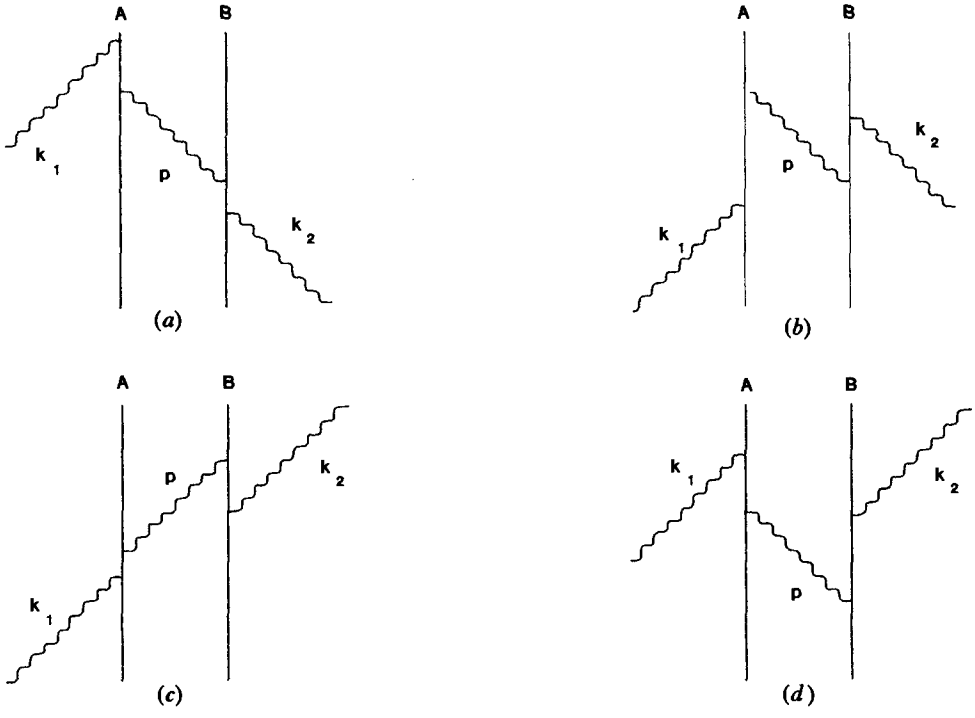

Figure 4. Typical time-order diagrams for cooperative two-photon processes, involving two molecules A and B. Figures (*a*) and (*b*) relate specifically to two-photon absorption, and (*c*) and (*d*) to Raman scattering.

second-order in the perturbation. These terms are found to be directly responsible for synergistic processes at each molecular centre. The derivation of the desired time-evolution operator thus becomes a simple matter of applying second-order perturbation theory with the result that

$$U(t,0)=\frac{(\mathrm{i}\hbar)^{-2}}{2!}T\sum_{p,\varepsilon}\left[\int_0^t \mathrm{d}t_1 \int_0^t \mathrm{d}t_2 H^{\mathrm{A}}_{\mathrm{eff}}(\mathbf{k}_1;\mathbf{p},t_1)H^{\mathrm{B}}_{\mathrm{eff}}(\mathbf{k}_2;\mathbf{p},t_2)\right]$$
$$=\frac{(\mathrm{i}\hbar)^{-4}}{4!}T\left[\int_0^t \mathrm{d}t_1 \int_0^t \mathrm{d}t_2 \int_0^t \mathrm{d}t_3 \int_0^t \mathrm{d}t_4 \right.$$
$$\left. \times H^{\mathrm{A}}_{\mathrm{int}}(\mathbf{k}_1,t_1)H^{\mathrm{A}}_{\mathrm{int}}(\mathbf{p},t_2)H^{\mathrm{B}}_{\mathrm{int}}(\mathbf{p},t_3)H^{\mathrm{B}}_{\mathrm{int}}(\mathbf{k}_2,t_4)\right], \tag{9}$$

where $H_{\mathrm{eff}}(\mathbf{k};\mathbf{p},t_1)$ and so on are the Heisenberg operator forms of

$$H^{\mathrm{A}}_{\mathrm{eff}}(\mathbf{k}_1;\mathbf{p})=-\mathrm{i}[S^{\mathrm{A}}(\mathbf{k}_1,\lambda),H^{\mathrm{A}}_{\mathrm{int}}(\mathbf{p},\varepsilon)], \tag{10}$$

$$H^{\mathrm{B}}_{\mathrm{eff}}(\mathbf{k}_2;\mathbf{p})=-\mathrm{i}[S^{\mathrm{B}}(\mathbf{k}_2,\lambda'),H^{\mathrm{B}}_{\mathrm{int}}(\mathbf{p},\varepsilon)], \tag{11}$$

where S^{A} and S^{B} are the generators for sites A and B respectively, defined in terms of the commutator relation

$$\mathrm{i}[S^{\mathrm{A}}(\mathbf{k}_1,\lambda),H_0]+\mathrm{i}[S^{\mathrm{B}}(\mathbf{k}_2,\lambda'),H_0]=H^{\mathrm{A}}_{\mathrm{int}}(\mathbf{k}_1,\lambda)+H^{\mathrm{B}}_{\mathrm{int}}(\mathbf{k}_2,\lambda'), \tag{12}$$

where H_0 represents the complete system Hamiltonian in the absence of any radiation–molecule perturbation term. Operating on either side of equations (10) and (11) with the initial and final state vectors for the system we find that the matrix element for the effective Hamiltonian at each molecular centre for the transition $|\mathrm{i}\rangle \rightarrow |\mathrm{f}\rangle$ is simply

$$\langle \mathrm{f}| H^{\mathrm{A}}_{\mathrm{eff}}(\mathbf{k}_1; \mathbf{p})|\mathrm{i}\rangle = -\varepsilon_0^{-2}\alpha^{\mathrm{A}}_{ij}(k_1)\mathbf{d}^{\perp}_j(\mathbf{p})\mathbf{d}^{\perp}_i(\mathbf{k}_1), \tag{13}$$

$$\langle \mathrm{f}| H^{\mathrm{B}}_{\mathrm{eff}}(\mathbf{k}_2; \mathbf{p})|\mathrm{i}\rangle = -\varepsilon_0^{-2}\alpha^{\mathrm{B}}_{ij}(k_2)\mathbf{d}^{\perp}_i(\mathbf{p})\mathbf{d}^{\perp}_j(\mathbf{k}_2). \tag{14}$$

The rank-2 tensors appearing in equations (13) and (14) are defined as

$$\alpha^{\mathrm{A}}_{ij}(k_1) = \sum_r \left(\frac{\mu_i^{\alpha r}\mu_j^{r0}}{E_{r\alpha} + \hbar c k_1} + \frac{\mu_j^{\alpha r}\mu_i^{r0}}{E_{r0} - \hbar c k_1} \right), \tag{15}$$

$$\alpha^{\mathrm{B}}_{ij}(k_2) = \sum_r \left(\frac{\mu_j^{\beta r}\mu_i^{r0}}{E_{r\beta} \pm \hbar c k_2} + \frac{\mu_i^{\beta r}\mu_j^{r0}}{E_{r0} \mp \hbar c k_2} \right). \tag{16}$$

Here and through the paper upper signs relate to TPA and lower signs to RS. The asymmetry in defining equations (15) and (16) arises in the choice of generator, which for simplicity we elect to be a function of the real photon parameters. The tensors $\alpha^{\mathrm{A}}_{ij}(k)$ and $\alpha^{\mathrm{B}}_{ij}(k)$ are clearly equivalent for the case of TPA. For Raman scattering, the equivalence of the two tensors is best illustrated in the long-range limit where the photon scattered at A assumes a real character. With $|\alpha\rangle = |0\rangle$ for example, then energy conservation demands that $E_{\beta 0} = \hbar c(k_1 - k_2)$. Substitution of this result into the energy denominators of equation (16) replicates the result in equation (15). Despite the similarity in form of the tensors for TPA and RS, it should be borne in mind that the excited states α and β are vibronic in the first case but vibrational in the second. In fact application of the Born–Oppenheimer wavefunction expansion in the latter case, together with the usual Placzek approximations [14] results in index symmetry in non-resonant cases. In previous work on cooperative TPA [5] results are expressed in terms of the molecular tensors $\mathbf{S}_{ij}(k_n) = -\alpha_{ij}(k_n)$, and to avoid confusion, the **S** tensors are used below whenever specifically referring to cooperative TPA.

The probability amplitude $c_{\mathrm{fi}}(t)$ for the process is obtained by substitution of equations (9)–(16) into equation (5). Carrying out the necessary time integrations, and performing the summation over the polarizations of the virtual states, leads to the following result involving only four terms corresponding to the *contracted* time-order diagrams shown in figure 5;

$$\begin{aligned} c_{\mathrm{fi}}(t) = {} & \frac{\exp[\mathrm{i}(\mp \mathbf{k}_2 \cdot \mathbf{R}_{\mathrm{b}} - \mathbf{k}_1 \cdot \mathbf{R}_{\mathrm{a}})]}{4\varepsilon_0^2 V^2} [n_1 n_2' k_1 k_2]^{1/2} \alpha^{\mathrm{A}}_{ij}(k_1)\alpha^{\mathrm{B}}_{kl}(k_2) e_i(\mathbf{k}_1(\bar{e}_1(\mathbf{k}_2) \\ & \times \sum_{p=0}^{\infty} p(\delta_{jk} - \hat{p}_j\hat{p}_k) \Bigg\{ \frac{\{\exp[\mathrm{i}ct(K_\alpha + K_\beta)] - 1\}\exp(\mathrm{i}\mathbf{p}\cdot\mathbf{R})}{(K_\alpha + K_\beta)(K_\beta + p)} \\ & - \frac{\{\exp[\mathrm{i}ct(K_\alpha - p)] - 1\}\exp(\mathrm{i}\mathbf{p}\cdot\mathbf{R})}{(K_\alpha - p)(K_\beta + p)} + \frac{\{\exp[\mathrm{i}ct(K_\alpha + K_\beta)] - 1\}\exp(-\mathrm{i}\mathbf{p}\cdot\mathbf{R})}{(K_\alpha + K_\beta)(K_\alpha + p)} \\ & - \frac{\{\exp[\mathrm{i}ct(K_\beta - p)] - 1\}\exp(-\mathrm{i}\mathbf{p}\cdot\mathbf{R})}{(K_\beta - p)(K_\alpha + p)} \Bigg\}. \end{aligned} \tag{17}$$

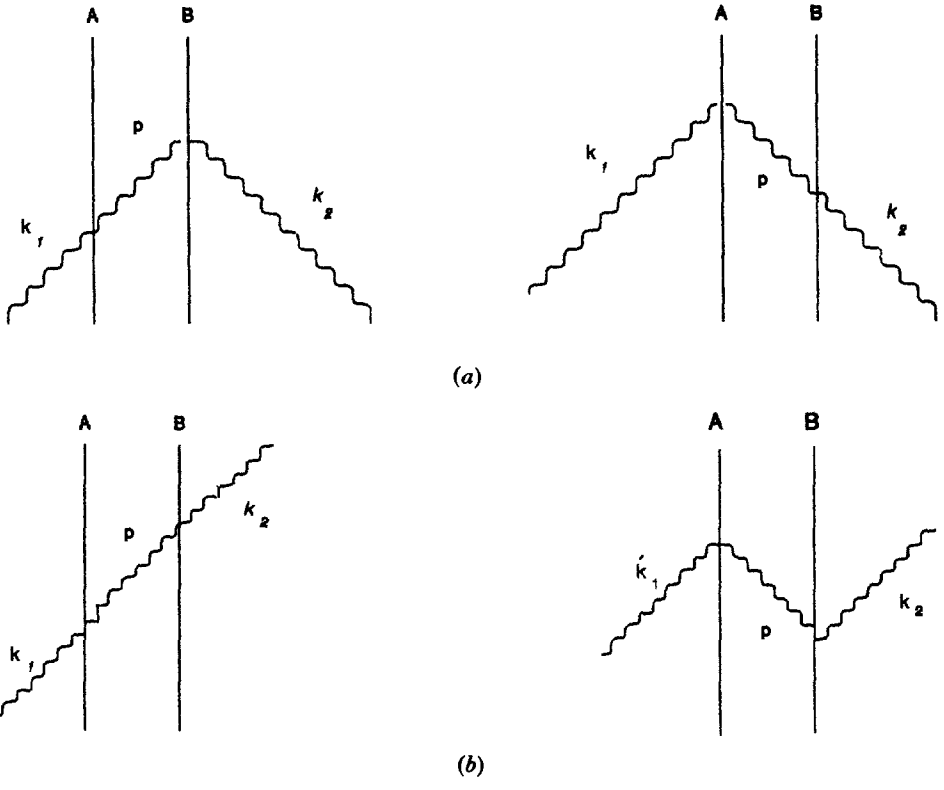

Figure 5. The contracted time-order diagrams for (*a*) cooperative two-photon absorption, and (*b*) cooperative Raman scattering.

Here $n_2' = n_2$ for synergistic two-photon absorption, and $n_2' = 1$ for Raman scattering. The vector $\mathbf{R} = (\mathbf{R}_b - \mathbf{R}_a)$ is the intermolecular separation vector that defines the location of centre B with respect to A, and the quantities K_α and K_β are defined as

$$K_\alpha = \frac{E_{\alpha 0} - \hbar c k_1}{\hbar c}, \tag{18}$$

$$K_\beta = \frac{E_{\beta 0} \pm \hbar c k_2}{\hbar c}. \tag{19}$$

In the above equations (18) and (19), it is assumed that for Raman scattering the photon of frequency ω_1 is annihilated at site A, and that the scattered photon is created at site B. For the TPA process, it is assumed that the photon annihilated at site B is greater in energy than the final state ($E_{\alpha 0} < \hbar\omega_1$), whilst $E_{\beta 0} > \hbar\omega_2$. Thus $K_\alpha < 1$ and $K_\beta > 1$. In order to simplify equation (17) the summation over the virtual modes is converted to an integral in p-space according to the prescription [15]

$$\sum_{p=0}^{\infty} \Rightarrow \frac{V}{8\pi^3} \int_{-\infty}^{\infty} \mathrm{d}^3 p. \tag{20}$$

Resorting to spherical polar coordinates, and carrying out angular integrations, gives

$$c_{fi}(t)=\frac{\exp[i(\pm\mathbf{k}_2\cdot\mathbf{R}_b-\mathbf{k}_1\cdot\mathbf{R}_a)]}{16\pi^2\varepsilon_0^2V}[n_1n_2'k_1k_2)^{1/2}\alpha_{ij}^A(k_1)\alpha_{kl}^B(k_2)e_i(\mathbf{k}_1)\bar{e}_l(\mathbf{k}_2)$$
$$\times(-\nabla^2\delta_{jk}+\nabla_j\nabla_k)\int_0^\infty\frac{\sin(pR)}{iR}\left\{\frac{\exp[ict(K_\alpha+K_\beta)]-1}{(K_\alpha+K_\beta)(K_\beta+p)}\right.$$
$$-\frac{\exp[ict(K_\alpha-p)]-1}{(K_\alpha-p)(K_\beta+p)}+\frac{\exp[ict(K_\alpha+K_\beta)]-1}{(K_\alpha+K_\beta)(K_\alpha+p)}$$
$$\left.-\frac{\exp[ict(K_\alpha-p)]-1}{(K_\beta-p)(K_\alpha+p)}\right\}dp. \tag{21}$$

The integrals in p-space can now be evaluated by noting that in timescales beyond the femtosecond region, only processes on the energy shell ($K_\alpha=-K_\beta$) contribute. This simply reflects the fact that energy conservation must be obeyed as the sampling time $t\to\infty$; this becomes evident when a summation over final states is conducted. On the energy shell, it is possible to reveal a hidden symmetry in the integrands by changing the variable of integration from p to $-p$ in some of the above integrals. In so doing, it is possible to show that

$$\int_0^\infty\frac{\sin(pR)}{iR}\left\{\frac{\exp[ict(K_\alpha+K_\beta)]-1}{(K_\alpha+K_\beta)(K_\beta+p)}-\frac{\exp[ict(K_\alpha-p)]-1}{(K_\alpha-p)(K_\beta+p)}\right.$$
$$\left.+\frac{\exp[ict(K_\alpha+K_\beta)]-1}{(K_\alpha+K_\beta)(K_\alpha+p)}-\frac{\exp[ict(K_\beta-p)]-1}{(K_\beta-p)(K_\alpha+p)}\right\}dp$$
$$=\int_{-\infty}^\infty\frac{\sin(pR)}{iR}\left\{\frac{\exp[ict(K_\alpha+K_\beta)]-1}{(K_\alpha+K_\beta)(K_\beta+p)}+\frac{1}{(K_\alpha-p)(K_\beta+p)}\right\}dp$$
$$-\int_0^\infty\frac{\sin(pR)}{iR}\left\{\frac{\exp[ict(K_\alpha-p)]}{(K_\alpha+p)(K_\beta-p)}+\frac{\exp[ict(K_\beta-p)]}{(K_\beta-p)(K_\alpha+p)}\right\}dp. \tag{22}$$

Of the last two integrals the first term has no pole in the region of integration, and is highly oscillatory. This integral is very similar to that ignored in the Fermi Golden Rule treatment of the second-order matrix element. This term averages to zero over periods of ctp that are sufficiently large, and is therefore ignored. The fourth integrand has two simple poles in the region of integration, and cannot be ignored. Noting that the principal contribution to this integral arises from the poles, it is possible to extend the limits of integration to $(-\infty,\infty)$. The integral involved is then easily solved by taking the Cauchy principal part [16] leading to the following inherently causal result;

$$\left.\begin{aligned}c_{fi}(t)&=\frac{\exp[i(\pm\mathbf{k}_2\cdot\mathbf{R}_b-\mathbf{k}_1\cdot\mathbf{R}_a)}{8\pi^2\varepsilon_0^2V}[n_1n_2'k_1k_2]^{1/2}\alpha_{ij}^A(k)\alpha_{kl}^B(k')e_i(\mathbf{k})\bar{e}_l(\mathbf{k}')\\&\times(-\nabla^2\delta_{jk}+\nabla_j\nabla_k)\frac{1}{R}\frac{\pi\exp(iK_\beta ct)}{(K_\alpha+K_\beta)}\\&\times\{\exp[-iK_\alpha(R-ct)]-\exp[iK_\beta(R-ct)]\};\quad ct>R\\c_{fi}(t)&=0;\qquad R>ct.\end{aligned}\right\} \tag{23}$$

To obtain the rate requires that the time derivative of the probability for the transition be calculated. The probability is simply the modulus square of the probability amplitude, and hence the rate, Γ, is given by

$$\left.\begin{aligned}\Gamma_{fi}^{TPA}(t) &= \frac{(n_1 n_2' k_1 k_2)}{4\varepsilon_0^2 V^2}\alpha_{ij}^{A}(k_1)\alpha_{kl}^{B}(k_2)e_i(\mathbf{k}_1)\bar{e}_l(\mathbf{k}_2)\bar{\alpha}_{mn}^{A}(k_1)\bar{\alpha}_{op}^{B}(k_2)\bar{e}_m(\mathbf{k}_1)e_p(\mathbf{k}_2)\\ &\times(4\pi\varepsilon_0)^{-1}(-\nabla^2\delta_{jk}+\nabla_j\nabla_k)\frac{1}{R}(4\pi\varepsilon_0)^{-1}(-\nabla'^2\delta_{no}+\nabla_n'\nabla_o')\frac{1}{R'}\\ &\times\frac{ic}{(K_\alpha+K_\beta)}\{\exp[-iK_\alpha(R-ct)-iK_\beta(R'-ct)]\\ &\qquad-\exp[iK_\beta(R-ct)+iK_\alpha(R'-ct)]\}\\ &=|N_{fi}|^2\frac{ic}{(K_\alpha+K_\beta)}\{\exp[-iK_\alpha(R-ct)-iK_\beta(R'-ct)]\\ &\qquad-\exp[iK_\beta(R-ct)+iK_\alpha(R'-ct)]\}.\end{aligned}\right\}\quad(24)$$

The final stage in the calculation of the transition rate is to sum over an appropriate set of final states for the system, this being tantamount to assuming that transitions occur to a continuum of states. This procedure is different for cooperative RS and TPA. In the Raman case the final states summation can be converted to a familiar integral over the frequency of the scattered photon; this procedure is outlined elsewhere [8]. Here we concentrate upon the summation over final states for two-photon absorption, since this has not previously been explicitly performed.

In cooperative TPA the appropriate final states for the system are the molecular final states $|\alpha\rangle$ and $|\beta\rangle$. Thus two summations are strictly required, and the observed transition rate is therefore given by

$$\sum_\alpha\sum_\beta|N_{fi}|^2\frac{ic}{(K_\alpha+K_\beta)}\times\{\exp[-iK_\alpha(R-ct)-iK_\beta(R'-ct)]-\exp[iK_\beta(R-ct)+iK_\alpha(R'-ct)]\}.\quad(25)$$

By converting the summation over the $|\alpha\rangle$ states to an integral over K_α, it is possible to show that, in the long-timescale limit, the observed rate takes the form

$$\sum_\beta|N_{fi}|^2 2\pi\hbar c^2\exp[iK_\beta(R-R')]\rho_f^A(k_1+k_2-K_{\beta 0}),\quad(26)$$

where, in deriving this result, it is implicitly assumed that the molecular response tensors and the density of final states, ρ_f^A, for molecule A are stationary functions of K_α in the frequency region close to ω_1. Finally one recasts the summation over the final states of molecule B as an integral over K_β, with the result that the observed time-independent transition rate may be written as

$$\begin{aligned}\Gamma_{fi}^{TPA} &= 2\pi\hbar^2c^3|N_{fi}|^2\int\rho_f^A(k_1+k_2-k)\rho_f^B(k)\exp[i(k-k_2)(R-R')]\,dk\\ &=\frac{\pi I(k_1)I(k_2)}{2\varepsilon_0^2c}\int dk\,\rho_f^A(k_1+k_2-k)\rho_f^B(k)\\ &\times\left|S_{ij}^A(k_1)S_{kl}^B(k_2)e_i(\mathbf{k}_1)\bar{e}_k(\mathbf{k}_2)\right.\\ &\left.\times(4\pi\varepsilon_0)^{-1}(-\nabla^2\delta_{jl}+\nabla_j\nabla_l)\frac{1}{R}\exp[-i(k-k_2)R]\right|^2,\end{aligned}\quad(27)$$

where $I(k_n)$ represents the irradiance (power per unit cross-sectional area) of the laser beam for mode k_n. In cooperative Raman scattering it is more useful to cast the result in terms of a radiant scattering intensity $I_{fi}^{RS}(k_2)$, defined as the Raman scattering energy radiated in the direction of $\mathbf{k}'$ per unit solid angle per unit time:

$$I_{fi}^{RS}(\mathbf{k}') = \frac{I(k_1)\mathbf{k}_2^4}{(4\pi\varepsilon_0)^2}\alpha_{ij}^{A}(k_1)\alpha_{kl}^{B}(k_2)e_i(\mathbf{k}_1)\bar{e}_i(\mathbf{k}_2)\bar{\alpha}_{mn}^{A}(k_1)\bar{\alpha}_{op}^{B}(k_2)\bar{e}_m(\mathbf{k}_1)e_p(\mathbf{k}_2)$$
$$\times (4\pi\varepsilon_0)^{-1}(-\nabla^2\delta_{jk}+\nabla_j\nabla_k)\frac{1}{R}(4\pi\varepsilon_0)^{-1}(-\nabla'^2\delta_{no}+\nabla'_n\nabla'_o)\frac{1}{R'}$$
$$\times \exp[\mathrm{i}(K_{\beta 0}-k_2)(R-R')]. \tag{28}$$

Equations (27) and (28) represent the master equations for two-photon cooperative phenomena. Of specific interest in these equations are the virtual photon coupling tensors, which are essentially of identical form not only in the phenomena considered here, but also in other resonant excitation transfer processes [17]: its properties are analysed in the following section.

3. Virtual photon coupling tensor

In this section, the properties of virtual photon coupling are discussed in some detail. As noted in section 1 both cooperative and distributive TPA and RS are characterized by a coupling tensor of the form

$$(4\pi\varepsilon_0)^{-1}(-\nabla^2\delta_{jk}+\nabla_j\nabla_k)\frac{1}{R}\exp(\mathrm{i}KR) = V_{jk}(K,R)$$
$$= \frac{1}{4\pi\varepsilon_0 R^3}\{[(\delta_{jk}-3\hat{R}_j\hat{R}_k)$$
$$\times[\cos(KR)+KR\sin(KR)]$$
$$-(\delta_{jk}-\hat{R}_j\hat{R}_k)K^2R^2\cos(KR)]$$
$$+\mathrm{i}\{(\delta_{jk}-3\hat{R}_j\hat{R}_k)[\sin(KR)-KR\cos(KR)]$$
$$-(\delta_{jk}-\hat{R}_j\hat{R}_k)K^2R^2\sin(KR)\}\}. \tag{29}$$

The tensor essentially describes how the energy mismatch between molecular centres is mediated. It is often referred to as the virtual photon propagator [18], or tensor field [19]. This term is of direct interest since all properties of intermolecular coupling are manifest within it. Whilst $V_{jk}(K,R)$ is oscillatory in nature, the molecular energy transfer function $\mathrm{Re}(V_{jk}(K,R)\bar{V}_{no}(K,R))$, involved in all coupling terms which appears in the transition rate, is non-oscillatory and has the form

$$V_{jk}(K,R)\bar{V}_{no}(K,R) = \frac{1}{16\pi^2\varepsilon_0^2R^6}[(\delta_{jk}-3\hat{R}_j\hat{R}_k)(\delta_{no}-3\hat{R}_n\hat{R}_o)(1+K^2R^2)$$
$$-[(\delta_{jk}-3\hat{R}_j\hat{R}_k)(\delta_{no}-\hat{R}_n\hat{R}_o)$$
$$+(\delta_{jk}-\hat{R}_j\hat{R}_k)(\delta_{no}-3\hat{R}_n\hat{R}_o)]K^2R^2$$
$$+(\delta_{jk}-\hat{R}_j\hat{R}_k)(\delta_{no}-\hat{R}_n\hat{R}_o)K^4R^4. \tag{30}$$

In the limit where the intermolecular separation is small ($KR<1$) only the first term in the above expression contributes appreciably to the rate equations. Substitution of

this term into the master equations (27) and (28) simply gives the familiar induced-dipole–induced-dipole results for two-photon absorption and Raman scattering respectively.

In the long-range limit ($KR>1$) the last term in equation (30) becomes dominant. This result, which is transverse with respect to R, shows that the intermolecular coupling tensor describes the long-range propagation of a real photon between molecular centres. The limit therefore corresponds to a process where a real photon mediates the mismatch energy $E_{a0}-\hbar ck_1$ to B through a scattering mechanism at A. This photon then proceeds to a subsequent two-photon absorption or scattering process at site B. The quantum electrodynamical result given in equations (27) and (28) thus shows how multiple-body and induced-dipole–induced-dipole mechanisms are in fact merely the long- and short-range limits of a unified theory of cooperative two-photon processes, involving intermolecular virtual photon energy transfer.

For fluids, it is necessary to sum over all possible interacting pairs when arriving at an expression for the observed rate or intensity. In practice therefore, R may take any one of a continuum of values, and a distributional average for the ensemble is required. It can safely be assumed that pair interactions are negligible over distances greater than the width of the laser beam, and hence the number of potential interacting pairs separated by distance R within a beam interaction volume V_I is $V_I\rho^2(R)g(R)R^2\,\mathrm{d}R$, where $\rho(R)$ is the number density and $g(R)$ the pair correlation function for the fluid. In randomly oriented molecular fluids free of translational symmetry it is thus possible to show that only incoherent contributions to the scattering remain, with the molecular energy transfer function, $\mathrm{Re}\,[V_{jk}(K,R)\bar{V}_{no}(K,R)]$ effectively being replaced by [8];

$$4\pi V_I R^2\rho(R)g(R)V_{jk}(K,R)\bar{V}_{no}(K,R)\,\mathrm{d}R. \tag{31}$$

Thus the cooperative processes described by the master equations (27) and (28) are now described by [6, 8, 10]

$$\begin{aligned}\Gamma_{fi}^{TPA}=\frac{\pi^2 I(k_1)I(k_2)}{\varepsilon_0^2 c}V_I\rho^2\int \mathrm{d}k\,\rho_f^A(k_1+k_2-k)\rho_f^B(k)\int_{-\infty}^{\infty}\mathrm{d}R\,R^2 g(R)\\ \times\langle\langle\langle\{S_{ij}^A(k_1)S_{kl}^B(k_2)e_i(\mathbf{k}_1)e_k(\mathbf{k}_2)V_{jl}(K,R)\\ +[k_1\leftrightarrow k_2]\exp[-\mathrm{i}(\mathbf{k}_1+\mathbf{k}_2)\cdot\mathbf{R}]\}\{\bar{S}_{mn}^A(k_1)\bar{S}_{op}^B(k_2)e_m(\mathbf{k}_1)e_o(\mathbf{k}_2)\bar{V}_{np}(K,R)\\ +[k_1\leftrightarrow k_2]\exp[\mathrm{i}(\mathbf{k}_1+\mathbf{k}_2)\cdot\mathbf{R}]\}\rangle\rangle\rangle\end{aligned} \tag{32}$$

$$\begin{aligned}I_{fi}^{RS}(k')=\frac{I(k_1)k_2^4}{8\pi\varepsilon_0^2}V_I\rho^2\int_{-\infty}^{\infty}\mathrm{d}R\,R^2 g(R)\\ \times\langle\langle\langle\{\alpha_{ij}^A(k_1)\alpha_{kl}^B(k_2)e_i(\mathbf{k}_1)\bar{e}_l(\mathbf{k}_2)V_{jk}(K,R)\\ +[k_1\leftrightarrow k_2]\exp[-\mathrm{i}(\mathbf{k}_1+\mathbf{k}_2)\cdot\mathbf{R}]\}\{\bar{\alpha}_{mn}^A(k_1)\bar{\alpha}_{op}^B(k_2)\bar{e}_m(\mathbf{k}_1)e_p(\mathbf{k}_2)\bar{V}_{no}(K,R)\\ +[k_1\leftrightarrow k_2]\exp[\mathrm{i}(\mathbf{k}_1+\mathbf{k}_2)\cdot\mathbf{R}]\}\rangle\rangle\rangle,\end{aligned} \tag{33}$$

where the angular brackets $\langle\langle\langle\ \rangle\rangle\rangle$ reflect the fact that a series of three rotational averages is required to account for (i) the random orientation of the A, B pair with respect to the laboratory frame, (ii) the random orientation of A with respect to B, and (iii) the random orientation of B with respect to A [10].

In explicitly carrying out the necessary averaging it is found that virtual photon coupling is governed by a linear combination of the isotropic components of the term $\mathrm{Re}\,[V_{ij}(K,R)\bar{V}_{kl}(K',R)\hat{R}_m\hat{R}_n\hat{R}_o\hat{R}_p]$, derived by contraction with index permutational isomers of the quadruple Kronecker delta product $\delta_{ij}\delta_{kl}\delta_{mn}\delta_{op}$. Thus the rate of any synergistic process in molecular fluids involves terms of the general form

$$T^{(0)}_{ijklmnop}(K,K';R)=(V_{ij}(K,R)\bar{V}_{kl}(K',R)\hat{R}_m\hat{R}_n\hat{R}_o\hat{R}_p)^{(0)}, \tag{34}$$

where $K=K_\alpha$ as defined in equation (18), $K'=E_{\beta 0}-\hbar ck_1/\hbar c$, and the superscripted (0) indicates that the weight-0 (isotropic) part of the tensor must be taken. The rate contribution associated with each weight-0 isomer of $T_{ijklmnop}$ carries a spherical Bessel function $j_n(|\mathbf{k}_1\mp\mathbf{k}_2|R)$ of order n equal to the number of $\hat{\mathbf{R}}$ vectors contracted with $V_{ij}\bar{V}_{kl}$ [20]. Since for all physical processes the near-zone dominates the rate equations, j_0 is considerably larger in magnitude than higher order terms. The most significant rate contributions therefore result from terms in which the indices i, j, k and l are contracted together, giving the two molecular energy transfer functions $V_{jk}(K,R)\bar{V}_{jk}(K',R)$ and $V_{jj}(K,R)\bar{V}_{kk}(K',R)$. Special functional forms arise, however, in cases where $K=K'$. From equation (29) the required results are as follows:

$$V_{jk}(K,R)\bar{V}_{jk}(K,R)=\frac{1}{8\pi^2\varepsilon_0^2R^6}(3+K^2R^2+K^4R^4), \tag{35}$$

$$V_{jk}(K,R)\bar{V}_{jk}(K',R)=\frac{\exp[\mathrm{i}(K-K')R]}{8\pi^2\varepsilon_0^2R^6}(3-3\mathrm{i}(K-K')R+(3KK'-K^2-K'^2)R^2$$
$$+\mathrm{i}(K^2K'-KK'^2)R^3+K^2K'^2R^4), \tag{36}$$

$$V_{jj}(K,R)\bar{V}_{kk}(K,R)=\frac{K^4R^4}{4\pi^2\varepsilon_0^2R^6}, \tag{37}$$

$$V_{jj}(K,R)\bar{V}_{kk}(K',R)=\frac{K^2K'^2R^4}{4\pi^2\varepsilon_0^2R^6}\exp[\mathrm{i}(K-K')R]. \tag{38}$$

The cases where $K\neq K'$ occur only in processes where $E_{\alpha 0}\neq E_{\beta 0}$. Here contributions involving equations (36) and (38) arise through quantum mechanical interference between probability amplitudes for processes in which the photon $\hbar ck_1$ is annihilated at each of the sites A and B. It is interesting to note that such terms are characterized by range-dependences involving odd powers of R.

In the more common processes where $K=K'$ one only needs to consider the results given in equations (35) and (37). Such cases arise in all distributive mechanisms and in cooperative mechanisms where the two species A and B are chemically identical, as manifest in (i) mean-frequency two-photon absorption, and (ii) vibrational harmonic Raman scattering. The latter is quite distinct from Raman scattering involving an overtone frequency, where the oscillator is necessarily anharmonic. Here the distinction between single-centre vibrational overtone and bimolecular vibrational harmonic scattering can most readily be differentiated through their difference in Raman frequency shift. Of the two terms (35) and (37) it is clearly the former that is more important in the near-zone; thus for most processes the latter term may be neglected and attention focused upon $V_{jk}(K,R)\bar{V}_{jk}(K,R)$.

Terms of precisely the same form as the results (35) to (38), but with different K values given by $k_1\pm k_2$, arise in dealing with the distributive mechanisms. Here crucial differences occur in connection with the extent of their near-zone behaviour, determined by the energy mediated by the virtual photon. In both synergistic TPA

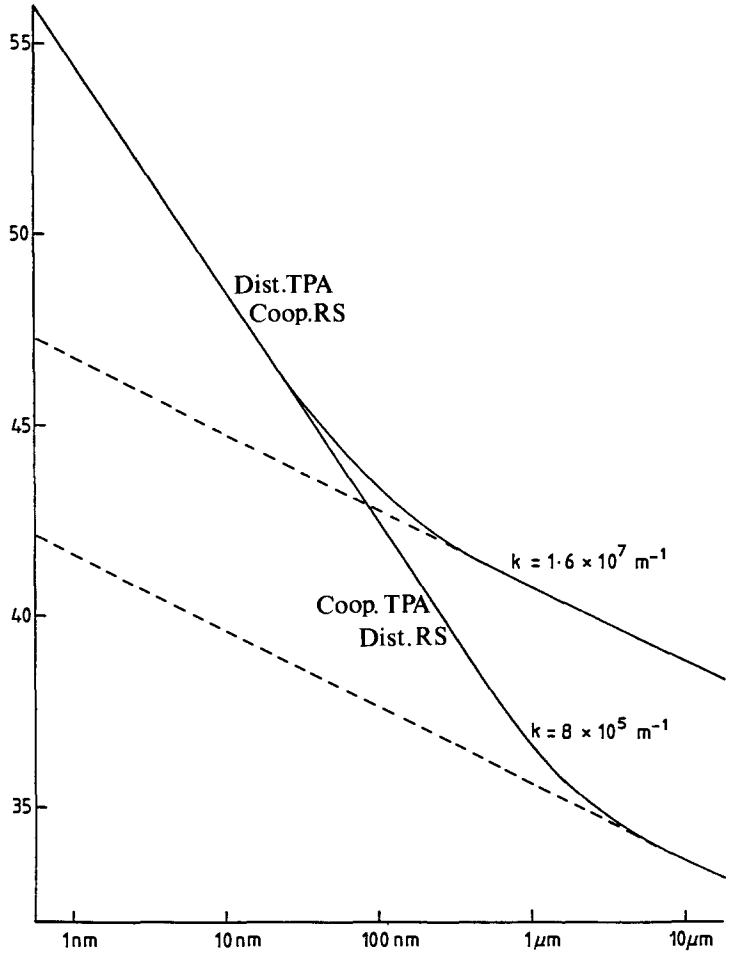

Figure 6. Typical log–log plot on an arbitrary vertical scale of the excitation transfer function $A(k, R)$ against intermolecular separation.

and RS the cooperative and distributive mechanisms are associated with very different coupling frequencies. For TPA the cooperative mechanism involves transfer of an energy difference typically equivalent to a molecular vibrational energy. By contrast the distributive mechanism involves transfer of an electronic energy. For RS, however, it is the distributive mechanism which conveys a vibrational energy and the cooperative mechanism an electronic energy [21].

Figure 6 illustrates the implications of this point with a log–log plot of the general function $V_{ij}(K, R)\bar{V}_{ij}(K, R)$ which occurs in all triply-averaged rate equations. The upper curve is plotted for a value of $K = 1{\cdot}6 \times 10^{7}\,\mathrm{m}^{-1}$, corresponding to conveyance of an electronic energy $E_{\beta 0}$ with a wavelength of about 400 nm. The lower curve with $K = 8 \times 10^{5}\,\mathrm{m}^{-1}$ corresponds to a mechanism where only an electronic energy *difference* (nominally $E_{\beta 0}/20$) is conveyed; here the difference equates to a vibrational energy with a wavenumber of around $1250\,\mathrm{cm}^{-1}$. At short distances the two graphs are indistinguishable and display the near-zone R^{-6} dependence. However, the

extent of the near-zone for the former case is much shorter, with the limiting far-zone R^{-2} behaviour already established at $R=1\,\mu m$; for the latter case far-zone behaviour obtains at $R=10\,\mu m$. The result of this difference is that the long-range rates (which vary with K^4) differ by a factor of $(20)^4=160\,000$ in favour of the distributive mechanism for synergistic TPA and the cooperative mechanism in RS [21].

4. Conclusion

In this paper, the characteristics of synergistic two-photon processes have been outlined in some detail. Whilst the theory expounded above shows that these effects are weaker than the single-centre contributions, certain novel features of the bimolecular processes should readily lead to an identification of the corresponding effects in TPA and RS spectra.

Synergism may first be characterized through the appearance of novel bands in a two-photon spectrum corresponding to simultaneous electronic, or vibrational, excitations. In TPA it is noted that one interesting effect would be the manifestation of mean-frequency absorption, whilst in RS it should be possible to identify combination bands, either as a result of simultaneous excitation of different vibrational modes in two distinct molecules, or by the appearance of vibrational second harmonics. In the case where the synergistic effect is purely intermolecular in nature, the unique nonlinear density and pressure characteristics of the bands in the spectrum should be readily identifiable.

Synergistic TPA may also lead to anomalous absorption in *single*-photon absorption experiments involving white or broadband light, such as the ultrafast laser supercontinuum [7]. This phenomenon, whereby molecular pairs synergistically absorb photons whose energy sum equals twice the transition energy for each molecule, should lead to a modification of the normal Beer–Lambert exponential decay law. The modification involves the addition of a term involving the frequency autocorrelation of the light, and should be manifest in a decrease in the apparent width of many lines in the absorption spectrum; in fact the Lorentzian linewidth of the synergistic process is readily shown to be approximately 0·64 times the ordinary absorption linewidth. Other types of optical nonlinearity which modify the form of any single-photon absorption spectrum are generally distinguishable by higher degrees of nonlinearity in the incident light intensity. Thus not only intensity-dependent lineshapes or extinction coefficients but also the appearance of ostensibly extraneous spectral lines may all be attributable to the effects of synergistic two-photon absorption.

Synergism may also occur within individual molecules or complexes. Here sites A and B will refer to otherwise uncoupled chromophores in a large molecule, a van der Waal's complex or a solvation complex, for example. In such systems it can be demonstrated that optical synergism is associated with gyrotropic effects. This is important since it demonstrates how one achiral centre can confer chirality upon another through their dissymmetric displacement with respect to each other. Where chiral effects occur in individual chiral centres, they are due to contributary interactions of magnetic-dipole character. However the detailed theory of both cooperative and distributive effects shows that both circular dichroism and circular differential scattering are a natural consequence of synergism, even in the local electric-dipole approximation, so long as the chromophores are dissymmetrically juxtaposed. The most interesting feature of these effects is their linear dependence

on R in the near-zone. Since circular dichroism or differential scattering in achiral sites can only occur as a result of synergism, use of this relatively simple technique provides another means of unambiguously identifying the effect.

In assessing the significance of the theoretical results presented above, it is useful to have some idea of the magnitude of the quantities involved. Although as noted above, synergistic effects in TPA are now experimentally well documented, neither experiment nor *ab initio* calculations have yet been performed to provide quantitative values for the various tensor parameters involved in the rate equations. Estimation of the more general significance of many of the results presented earlier must therefore proceed from a different basis. As shown in early work on cooperative photoabsorption [9, 10], neighbouring molecules can be expected to display a synergistic rate approaching the rate of a two-photon process in individual molecules, a result which is more readily calculated: this can be argued as follows.

A comparison of the short-range limit of the rate equation for *cooperative* absorption and the corresponding rate equation for normal two-photon absorption shows that the former contains an additional factor of the order of $\rho = S^{a0}/\varepsilon_0 R^3$. Far from accidental resonances, the molecular tensor should be similar in magnitude to the polarizability, since it is constructed in the same way from products of electric dipole transition moments divided by energy mismatch factors. Molecular polarizabilities, at least for small molecules, have well documented values, and are mostly similar in magnitude to the cube of molecular diameter. Hence when R represents a nearest-neighbour distance, the factor ρ approaches the value of unity, and the cooperative rate is comparable with that of a conventional two-photon process. Similar reasoning can be applied to the case of the *distributive* mechanism.

In the light of these arguments it is perhaps not surprising that synergistic effects are now being reported in two-photon spectroscopy. The explicit characterization of synergistic single-beam two-photon absorption has recently been described by Fajardo *et al.* [22, 23] in connection with a study of laser-induced charge transfer process. Here it has been possible to make a clear distinction from *sequential* absorption on the basis of kinetic considerations, and it has been show that synergistic TPA is the only mechanism which can satisfactorily account for all the experimental observations.

Acknowledgment

N.P.B. gratefully acknowledges funding from the United Kingdom S.E.R.C.

References

[1] Craig, D. P., and Walmsley, S. H., 1964, *Excitons in Molecular Crystals* (New York: Benjamin).
[2] Rios Leite, J. R., and De Araujo, C. B., 1980, *Chem. Phys. Lett.*, **73**, 1.
[3] White, J. C., 1981, *Optics Lett.*, **6**, 242.
[4] Andrews, D. L., and Hopkins, K. P., 1987, *J. chem. Phys.*, **86**, 2453.
[5] Andrews, D. L., and Hopkins, K. P., 1988, *J. chem. Phys.*, **89**, 4461.
[6] Andrews, D. L., and Hopkins, K. P., 1988, *J. Molec. Struct.*, **175**, 141.
[7] Andrews, D. L., 1988, *Phys. Rev.* A, **38**, 5129.
[8] Andrews, D. L., and Blake, N. P., 1990, *Phys. Rev.* (to be published).
[9] Andrews, D. L., and Harlow, M. J., 1983, *J. chem. Phys.*, **78**, 1088.
[10] Andrews, D. L., and Harlow, M. J., 1984, *J. chem. Phys.*, **80**, 4753.
[11] Power, E. A., and Zienau, S., 1959, *Phil. Trans. R. Soc. Lond.* A, **251**, 427.
[12] Gburski, S., Samios, J., and Dorfmüller, Th., 1987, *J. chem. Phys.*, **86**, 383.
[13] Langhoff, P. W., Epstein, S. T., and Karplus, M., 1974, *Rev. mod. Phys.*, **44**, 602.

[14] PLACZEK, G., and TELLER, E., 1938, *Z. Phys.*, **83,** 209.
[15] CRAIG, D. P., and THIRUNAMACHANDRAN, T., 1984, *Molecular Quantum Electrodynamics* (London: Academic), p. 147.
[16] CHURCHILL, R. V., BROWN, J. W., and VERHEY, R. F., 1974, *Complex Variables and Applications*, third edition (London: McGraw-Hill), p. 182.
[17] ANDREWS, D. L., and SHERBORNE, B. S., 1987, *J. chem. Phys.*, **86,** 4011.
[18] KEATING, S. P., 1983, *Molec. Phys.*, **48,** 655.
[19] CRAIG, D. P., and THIRUNAMACHANDRAN, T., 1983, *Phys. Rev.* A, **28,** 2663.
[20] ANDREWS, D. L., and HARLOW, M. J., 1984, *Phys. Rev.* A, **29,** 2796.
[21] ANDREWS, D. L., 1989, *Chem. Phys.*, **135,** 195.
[22] FAJARDO, M. E., and APKARIAN, V. A., 1987, *Chem. Phys. Lett.*, **134,** 55.
[23] FAJARDO, M. E., and APKARIAN, V. A., 1986, *J. chem. Phys.*, **85,** 5660.